Histol Histopathol (1997) 12: 769-779

Histology and Histopathology

Invited Review

Immunocytochemical localization of the vacuolar H^+-ATPase pump in the kidney

B. Bastani

Division of Nephrology, St. Louis University Health Sciences Center, St. Louis, MO, USA

Summary. In this article we review immunocytochemical localization studies using a monoclonal antibody raised against the 31 kD subunit of bovine H^+-ATPase, and indirect immunofluorescent staining. In the proximal tubules there is intense H^+-ATPase staining along the brush borders of S1 and S2, and linear subvillar invagination staining in S1, S2, and S3 segments. In the thick ascending limb of the loop of Henle there is a mild to moderate degree apical cytoplasmic vesicular staining. In distal convoluted tubule there is mild to moderate degree of H^+-ATPase staining which is sharply delineated along the luminal plasma membrane. In the connecting tubule, the connecting tubule cells show mild to moderate luminal membrane and apical cytoplasmic vesicular staining, and the intercalated cells demonstrate prominent H^+-ATPase staining which is polarized to either apical or basolateral pole or distributed diffusely throughout the cell. In the cortical collecting duct the principal cells show minimal or no staining while the intercalated cells show very bright H^+-ATPase staining with 6 identifiable morphologic subtypes based on polarization of the pump to apical or basolateral poles, and the degree of polarization (well polarized or poorly polarized). In the medullary collecting duct the principal cells show no staining and the intercalated cells show prominent H^+-ATPase staining only in the apical pole. We also describe adaptive responses to different physiologic manipulations e.g. chronic oral acid loads, chronic respiratory acidosis, remnant kidney model, chronic desoxycorticosterone (DOCA) administration, and chronic potassium depletion diet. Moreover, we compare the immunocytochemical localization of the H^+-ATPase pump of rabbit and kidneys.

Key words: Acid-base, Proton, H^+-ATPase, Immunocytochemistry, Intercalated cell, Kidney

Offprint requests to: Dr. Bahar Bastani, M.D., Associate Professor of Internal Medicine, Division of Nephrology, St. Louis University Health Sciences Center, 3635 Vista Avenue, 9N–FDT, St. Louis, MO 63110, USA

Introduction

In order to maintain normal acid-base homeostasis the kidneys must regenerate the bicarbonate lost to daily acid production from metabolism of dietary proteins (net acid excretion). Moreover, the kidneys increase acid secretion during increased intake or generation of acid, and increase excretion of bicarbonate during net alkali intake. The vacuolar H^+-ATPase pump is responsible for 30-40% of proton secretion in the proximal tubule and the majority of proton secretion in the distal nephron.

The vacuolar H^+-ATPase is an electrogenic proton pump which was first discovered in membranes from turtle urinary bladder, a model for mammalian collecting duct, with unique properties of resistance to mitochondrial ATPase inhibitors (oligomycin and azide) and extreme sensitivity to sulfhydril agent N-ethylmaleimide (NEM) (Gluck et al., 1982). This pump has further been characterized to be vanadate and ouabain resistant but to be very sensitive to bafilomycin A1, at the nanomolar range. A similar proton pump has subsequently been found in a wide range of intracellular organelles (e.g., lysosomes, Golgi membranes, endoplasmic reticulum, endosomes, and clathrin-coated vesicles), and so has been named the vacuolar-type H^+-ATPase pump. The H^+-ATPase pumps purified from different mammalian and plant sources or from different intracellular membrane compartments have been found to have remarkably similar structures. They are large-molecular weight heteromultimeric proteins with Mr ~ 600,000 daltons and at least 8-10 different subunits. They have a "club" or "stud" like overall structure and are composed of a cytosolic domain (V1) and a transmembrane proteolipid domain (V0). The V1 domain contains at least five different polypeptide chains which include: A subunit (Mr ~ 70 kD, 3 copies, contains catalytic ATP binding site), B subunit (Mr ~ 56 kD, 3 copies, has regulatory function), and several additional polypeptide subunits (C subunit, Mr ~ 42 kD; D subunit, Mr ~ 33 kD; E subunit, Mr ~ 31 kD; one copy of each). The latter subunits (C, D, and E) form a stalk, connecting the "catalytic head" of the H^+-ATPase (A and B subunits) to the transmembrane V0 domain (Mr ~

15-17 kD, 6 copies, forming a transmembrane proton channel) (Gluck et al.,1991; Forgac, 1992; Gluck, 1993). It is now believed that vacuolar H^+-ATPase exists as a family of enzymes with differences in their structure and function (Wang and Gluck, 1990; Gluck, 1992, 1993; Hemken et al., 1992; Nelson et al., 1992). There is evidence that subtle differences in structure of some subunits may account for the tissue, cell and organelle-specific expression of different isoforms. These isoforms are responsive to different regulatory machinery and are involved in endocytic/exocytic pathways (all eukaryotic cells) and transepithelial proton transport (renal proximal tubule and intercalated cells).

In this article, we present immunocytochemical localization of the vacuolar H^+-ATPase pump along the nephron. For biochemical and ultrastructural localization studies, one may refer to several recently published excellent reports (Ait-Mohamed et al., 1986; Brown et al., 1988a; Garg, 1991; Hamm et al., 1991; Verlander et al., 1991, 1994; Doucet et al., 1993; Gluck et al., 1993).

Immunocytochemical methods

In the studies that we report, 2 mm thick kidney slices were fixed in B5 ($HgCl_2$, 0.22M; sodium acetate, 90 mM; formaldehyde, 3.7%) overnight. Four micrometer thick sections from paraffin blocked tissue were deparaffinized in Xylene solution, rehydrated in decreasing concentrations of ethanol, and serially incubated in Lugol's iodine solution, 5% sodium thiosulfate, and PBS (pH 7.4). To block non-specific binding, sections were incubated in blocking solution (10% calf serum, 10% goat serum, 1% polyethylene glycol [Mr, 20,000] in PBS) for 30 minutes. Sections were then incubated overnight with undiluted supernatant from hybridoma E-11 (primary antibody). Samples were subsequently rinsed in PBS, incubated in 1:50 (vol:vol) dilution of fluorescein isothiocyanate (FITC)-labeled goat anti-mouse secondary antibody, for 20 minutes. Sections were then rinsed in PBS and mounted in a fresh mixture of paraphenylene diamine (2 mg/ml) in 50% glycerol (vol:vol, in PBS). Slides were viewed with a Nikon Optiphot-2 Mercury epifluorescent microscope (Nikon Corp., Instrument Division, New York, USA).

The primary antibody used in these immunocytochemical studies was a monoclonal antibody (E11) raised against a 10 amino acid synthetic peptide derived from the predicted sequence of the carboxyl-terminus of the bovine H^+-ATPase 31kD subunit (generous gift of Dr. Stephen Gluck, Washington University School of Medicine, St. Louis, USA) (Hemken et al., 1992).

Proximal tubule

The proximal tubule (PT) has three morphologically and functionally distinct segments: S1, S2, and S3 segments. The S1 and initial one-half of the S2 segments constitute the proximal convoluted tubule (PCT) which resides in the cortex. The distal one-half of the S2, and the S3 segments constitute the straight segment (pars recta) which resides in the medullary rays in the cortex, and in the outer stripe of the outer medulla. The PT is responsible for reabsorption of approximately 80-90% of the filtered load of bicarbonate. In order for bicarbonate to be reabsorbed it has to be buffered to carbonic acid via active proton secretion. Although the Na^+:H^+ antiporter (NHE3) is the major mechanism for proton secretion in this segment (Alpern, 1990), a vacuolar type H^+-ATPase also present in the brush border membrane (Brown et al, 1988a; Simon and Burckhardt, 1990; Wang and Gluck, 1990; Bastani et al., 1994a,b) has been shown to contribute to up to 40% of the overall proximal proton secretion in the rat (Preisig et al., 1987; Bank et al., 1989; Turrini et al., 1989). A recent report has suggested that luminal Na^+:H^+ exchanger is predominately regulated by pH whereas H^+-ATPase is mainly regulated by bicarbonate and/or PCO_2 (Soleimani et al., 1995).

Immunocytochemical staining of the rat kidney reveals intense staining of brush borders in the PCT and a linear pattern of apical staining in the pars recta (Fig. 1). Previous ultrastructural studies using affinity purified rabbit antisera raised against 3 subunits (70 kD, 56 kD, 31 kD) of bovine kidney medulla have revealed that the brush border membrane staining in the S1 and S2 segments corresponds to the presence of H^+-ATPase along the inner surface of the brush border microvilli, and at the base of the microvilli (subvillar invaginations), while staining in the S3 segment is limited to the subvillar invaginations (Brown et al., 1988a). Moreover, the H^+-ATPase labeled subvillar invaginations were found to be distinct from clathrin-coated membranes (Brown et al., 1988a). Ultrastructurally, the brush border membrane staining is more prominent along the microvilli in S1, less prominent in S2, and almost absent in S3 (Brown et al., 1988a).

In the cortex of the rabbit kidney there is a minimal H^+-ATPase staining along the luminal membrane of the PCT cells, which corresponds to the pattern of subvillar invaginations seen in the pars recta of the rat, albeit at a much fainter degree (Fig. 5A).

Thick ascending limb of loop of henle

The thick ascending limb (TAL) begins at the junction of outer and inner medulla, transverses the inner and the outer stripes (medullary TAL) and enters the cortex (cortical TAL). The cortical TAL approaches its own glomerulus forming the macula densa and terminates within a millimeter beyond it. The TAL is responsible for reabsorption of approximately 5-10% of the filtered bicarbonate. Proton secretion in the TAL is via both Na^+:H^+ antiporter (80%) and the H^+-ATPase pump (20%) (Borensztein, 1991).

On immunocytochemical staining, there is a mild to moderate degree of apical cytoplasmic vesicular staining for H^+-ATPase present in both medullary and cortical

TAL (Fig. 2).

Distal convoluted tubule

The distal convoluted tubule (DCT) follows the cortical TAL shortly after macula densa and is responsible for reabsorption of 1-3% of the filtered load of bicarbonate. This segment is composed of a uniform cell type.

On immunocytochemical staining, there is a mild to moderate degree of H^+-ATPase staining at the luminal plasma membrane of the DCT cells (Fig. 1).

Connecting tubule

The connecting tubule (CNT) immediately follows the DCT in cortex. It is composed of two cell types: the CNT cells and the intercalated cells (IC). The CNT cells resemble the DCT cells in having a low level of vacuolar H^+-ATPase in their apical plasma membrane, and resemble the principal cells of the cortical collecting duct in expressing apical potassium and amiloride-sensitive sodium channels. The IC in the CNT are similar to their counterparts in the cortical collecting duct and exhibit the same morphologic and functional subclasses.

On immunocytochemical staining of the rat kidney, the CNT cells show mild to moderate degrees of luminal membrane and apical cytoplasmic vesicular staining. In contrast, IC demonstrate a prominent H^+-ATPase staining which may be more polarized to the apical pole, basolateral pole, or distributed diffusely throughout the cell (Fig.1).

Cortical collecting duct

The initial collecting tubules upon joining together form the cortical collecting ducts (CCD) in the medullary rays of the cortex. The cortical and medullary collecting ducts are responsible for reabsorption of the remaining 5-10% of the filtered bicarbonate, as well as, net acid excretion (generation of new bicarbonate which has been lost to the catabolism of dietary protein). The CCD plays a flexible role in the maintenance of acid-base balance. It responds to an acid-load with enhanced proton secretion, and responds to a bicarbonate-load with enhanced bicarbonate secretion (McKinney and Burg, 1977, 1978a,b; Lombard et al., 1983; Atkins and Burg, 1985). This segment is composed of two different cell types: the principal cells (PC) comprising ~ 60% of the cells, and the intercalated cells (IC) comprising the remaining ~ 40%. The PC express in their apical

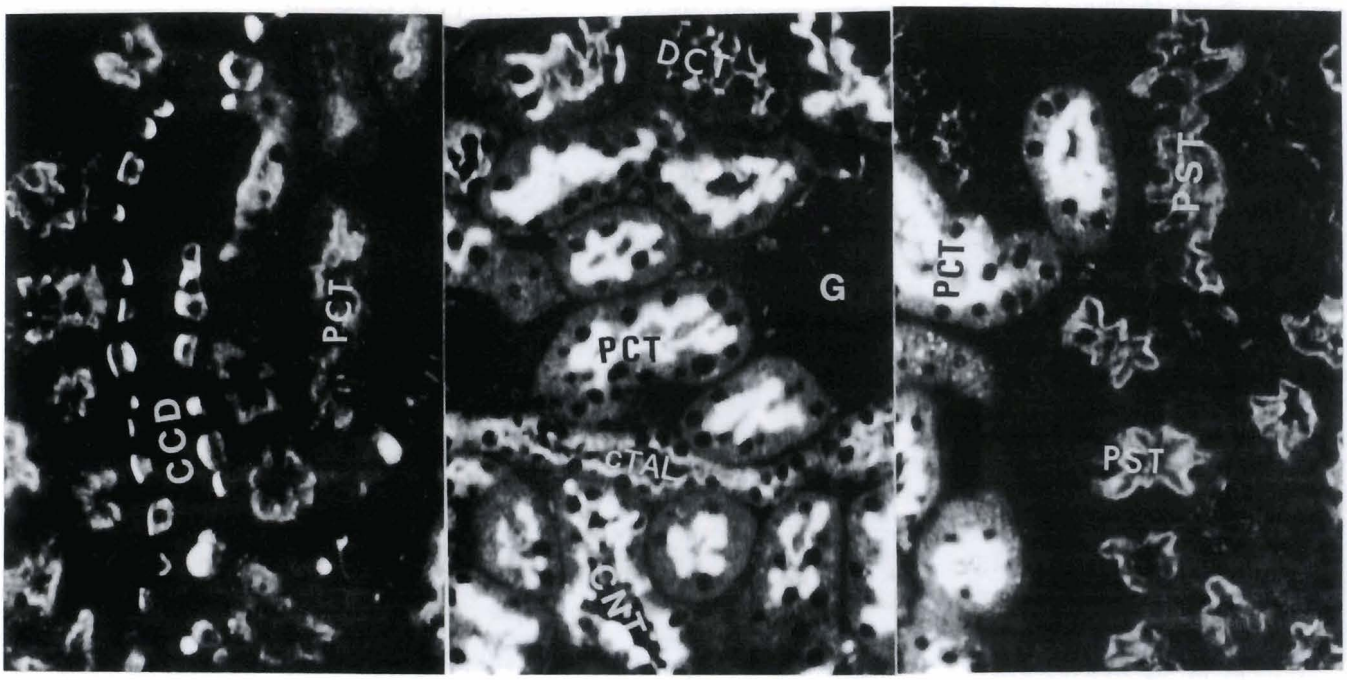

Fig. 1. Immunocytochemical staining of the rat kidney cortex using a monoclonal antibody against the 31kD subunit of H^+-ATPase as detailed in the text. The glomerulus (G) shows no staining. The proximal convoluted tubules (PCT) show intense staining in the brush borders and subvillar invaginations. The cortical thick ascending limb (cTAL) shows moderate apical cytoplasmic staining. The distal convoluted tubule (DCT) shows mild to moderate H^+-ATPase staining in the luminal plasma membrane. The connecting tubule (CNT) contains intercalated cells with prominant H^+-ATPase staining and CNT cells with moderate degrees of apical cytoplasmic H^+-ATPase staining. The cortical collecting duct (CCD) is composed of principal cells (PC) which show no H^+-ATPase staining and intercalated cells (IC) which show very bright staining for H^+-ATPase. The distribution of H^+-ATPase in the IC is either apical, basolateral, diffuse, or bipolar. Moreover, the cells with apical or basolateral staining for H^+-ATPase are either well polarized or poorly polarized. The proximal straight tubules (PST) show linear apical H^+-ATPase staining which correspond to the subvillar invaginations. x 310

membrane: amiloride-sensitive sodium channels, potassium channels, and aquaporin 2 water channels. In their basolateral membrane they express: Na^+,K^+-ATPase, $Na^+:H^+$ antiporter, and aquaporin 3 water channels. The PC are responsible for transepithelial sodium and water reabsorption, and potassium secretion, all of which are under the control of regulatory hormones. As a result of vectorial transepithelial sodium reabsorption, from lumen toward plasma, a lumen-negative voltage of -5 to -30 mV is generated in this segment. The IC are specialized cells which maintain dense arrays of the H^+-ATPase pump, in a polarized distribution, on the plasma membrane to implement net proton or bicarbonate secretion (Schuster et al., 1986; Brown et al., 1987, 1988a). The IC are responsible for both acid-base homeostasis and active potassium reabsorption. Because of the interspecies differences in the patterns and subtypes of IC, we will discuss the rat and rabbit CCD separately.

In the rat, there are at least two different subtypes of IC which differ significantly in morphologic and physiologic properties (Schuster et al., 1986; Brown et al., 1987, 1988a,b; Alpern et al., 1989; Bastani et al., 1991; Verlander et al., 1991; Bastani, 1995). The type A-IC (acid-secreting IC) express vacuolar H^+-ATPase in the apical pole. The H^+-ATPase is in both luminal plasma membrane and in a specialized intracellular tubulovesicular system (Brown et al., 1988b; Alpern et al., 1989; Verlander et al., 1991) from which additional H^+-ATPase containing membrane may be recruited to the luminal membrane upon appropriate physiological stimuli (Bastani, 1995; Schwartz and Al-Awqati, 1985). The type A-IC also express H^+,K^+-ATPase pump in their apical pole (Bastani, 1995). The bicarbonate which is generated in the cytoplasm as a result of proton secretion exits the basolateral membrane through a $Cl^-:HCO_3^-$ anion exchanger, a truncated form of red blood cell AE1 anion exchanger (band-3 protein) (Schuster et al., 1986; Verlander et al., 1988; Alpern et al., 1989; Brosius et al., 1989; Madsen et al., 1992). Ultrastructurally, type A-IC contain numerous microprojections (microplicae and microvilli) in their apical plasma membrane, abundant apical cytoplasmic tubulovesicular structures which contain ~10 nm diameter "studs", representing the H^+-ATPase pump, on their cytoplasmic face. They also contain abundant evenly distributed mitochondria, a centrally located nucleus, and an uncomplicated basolateral plasma membrane (Verlander et al., 1987). Based on ultrastructural features (Verlander et al., 1987), and H^+-ATPase immunocytochemistry in response to chronic acid-loads (Bastani et al., 1991), approximately 60 to 70% of IC in the CCD are type A (acid secreting).

The type B-IC which is designed for electroneutral chloride reabsorption and bicarbonate secretion, has an

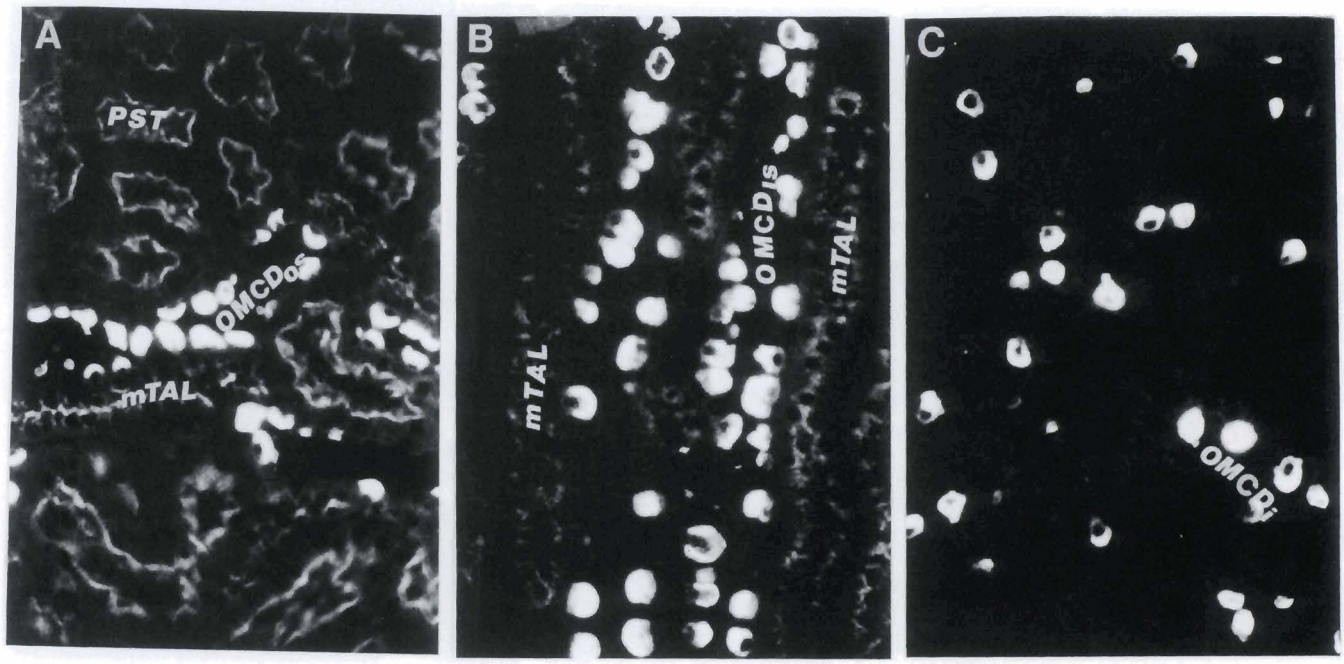

Fig. 2. Immunocytochemical staining of the rat kidney medulla using a monoclonal antibody against the 31 kD subunit of H^+-ATPase. **A.** The outer stripe of the outer medulla. The PST show linear apical H^+-ATPase staining corresponding to subvillar invaginations. The medullary thick ascending limb (mTAL) shows mild to moderate degree of stippled apical cytoplasmic H^+-ATPase staining. The outer medullary collecting duct (OMCDOS) is composed of PC with no detectable H^+- ATPase staining and IC which show prominent H^+-ATPase staining predominantly in the apical pole (type A-IC). **B.** The inner stripe of the outer medulla. The mTAL shows mild stippled apical cytoplasmic staining. The OMCDIS show PC with no staining at all and IC with prominent H^+-ATPase staining in the apical pole (type A-IC). **C.**In the initial one-third of the inner medullary collecting duct ($IMCD_I$) IC show prominent H^+-ATPase staining and comprise ~10% of the cells. PC show no H^+-ATPase staining and comprise the remaining ~90% of the cells. In the terminal two-thirds ($IMCD_T$) there is only one cell type, the IMCD cells, which show no H^+-ATPase staining (data not shown). x 310

apical Cl^-:HCO_3^- anion exchanger which is not reactive to antibodies raised against band-3 protein (Schuster et al., 1986; Alpern et al., 1989; Verlander et al., 1988). These cells acidify or alkalinize their cytosol after basolateral or luminal chloride removal, respectively, and on immunocytochemical staining show a basolateral, diffuse, or bipolar distribution of H^+-ATPase (Brown et al., 1988b; Alpern et al., 1989; Bastani et al., 1991). Ultrastructurally, they have a small and relatively smooth apical plasma membrane, extensive basolateral plasma membrane infoldings, eccentrically located nucleus, electron dense cytoplasm, numerous clustered mitochondria, and small vesicles that lack "studs" and are distributed throughout the cytoplasm (Verlander et al., 1987).

On immunocytochemical staining for H^+-ATPase, PC show minimal or no staining at all while IC show a very bright staining (Fig. 1). Six morphologic subtypes of IC can be identified in the CCD: 1) well polarized apically stained cells (WPA; H^+-ATPase staining limited to the apical region of the cell); 2) poorly polarized apically stained cells (PPA; H^+-ATPase staining accentuated in the apical region but also extending beyond the nucleus to the basal region); 3) well polarized basolaterally stained cells (WPB; H^+-ATPase staining is limited to the basolateral membrane of the cell); 4) poorly polarized basolaterally stained cells (PPB; H^+-ATPase staining accentuated in the basolateral region of the cell but also extending beyond the nucleus); 5) bipolar cells (BA) in which there is distinct staining of both basolateral and apical poles; 6) cells with diffuse H^+-ATPase staining throughout the cytoplasm (D), (Fig. 1). In normal control rats, 41% of IC show features of WPA, 25% PPA, 2% WPB, 17% PPB, 5% BA, and 10% D (Bastani et al., 1991). After oral acid-loading, the most obvious change was a steady increase in the percentage of WPA cells from ~45% to ~70% over the two week acid-loading period. This was accompanied by a decline in the percentages of PPA, D, and BA cells (Bastani et al., 1991). In the alkali-loaded animals, after a transient increase in WPA cells with a concomitant decrease in PPA cells on day 1, the percentage of PPA and WPA remained unchanged from control, throughout the two week experiment (Bastani et al., 1991). At several time points, the percentage of BA cells was significantly higher in the alkali-loaded rats (mean, 9%; range, 6.5-11%) when compared with the controls (mean, 5%; range, 3-6%). The percentage of WPB cells was always higher in the alkali-loaded than in the control animals (Bastani et al., 1991). We have found

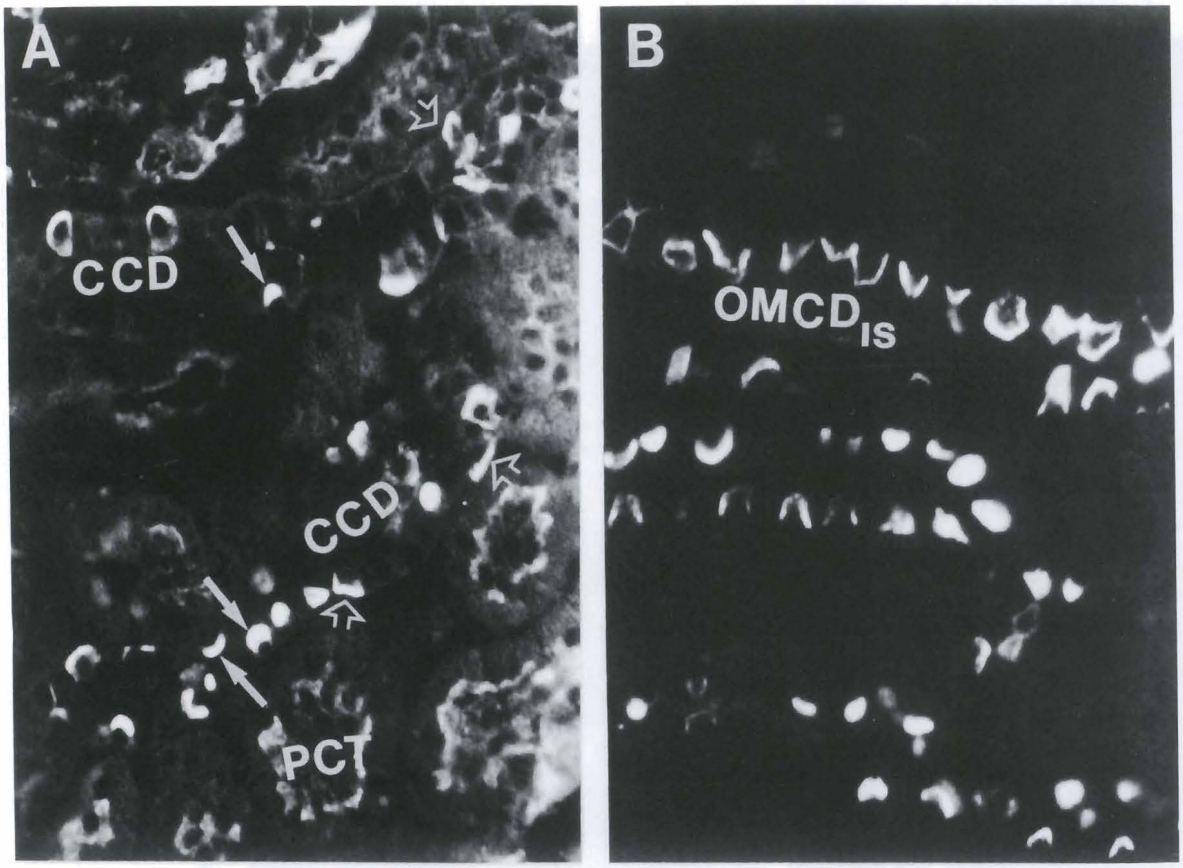

Fig. 3. Rats which had undergone 7/8 nephrecotmy (remnant kidney model) were studied at 1, 2, and 3 weeks. **A.** The CCD show a reduction in the percentage of IC and a concomitant increase in the percentage of PC. A higher percentage of IC show well polarized apical (WPA, solid arrow) and well polarized basolateral (WPB, hollow arrow) morphology. **B.** IC in the OMCDIS show a prominent luminal membrane staining (rim cells), with a concomitant reduction in the cytoplasmic vesicular pattern of H^+-ATPase staining. x 400

similar changes in H^+-ATPase distribution, albeit to a lesser degree in a model of chronic respiratory acidosis, and in models of chronic desoxycorticosterone (DOCA) administration, remnant kidney, and chronic K^+-depletion (Bastani et al., 1990, 1993; Bastani and Gluck, 1992). In the remnant kidney model, rats were subjected to 7/8 nephrectomy and were studied at 1, 2, and 3 weeks. We found significant increase in the percentages of WPA (36-48% vs. 15-27%) and WPB (6-12.5% vs. 1-3%) in the remnant vs. sham operated rats, respectively, over the three week study period (Fig. 3) (Bastani et al., 1990). We also found a significant increase in the percentage of PC, with a proportional decrease in IC (~33% vs. 42%, remnant vs. sham operated, respectively), in the CCD of the remnant kidneys (Bastani et al., 1990). In chronic (2 weeks) DOCA (Bastani and Gluck, 1992) administration and chronic (2 week) K^+-depleted diet (our unpublished preliminary observation, Fig. 4) we also found a significant increase in the percentages of WPA and WPB in the CCD.

The rabbit CCD is more complex since there is an axial heterogeneity of cell types along the length of the CCD, from superficial cortex toward deeper cortex (medullary rays), and there are IC that can not be easily classified into type A or type B variety. In contrast to the rat CCD in which distinct type A- and type B-IC are easily identified by morphologic appearance, the rabbit CCD exhibits a wide range variation in features of IC, without clear morphologic separation into discrete cell types. Moreover, the rabbit type B-IC binds peanut lectin (PNA) apically, a property which has been used in many studies to identify this cell type (Schuster, 1991). Based on PNA binding, anti-band-3 immunocytochemistry, and electrophysiological properties of individual IC, 70- 80% of ICs in the rabbit CCD have been identified as type B (Schuster et al., 1986; Schwartz et al., 1988; Muto et al., 1990). Moreover, a study using carbonic anhydrase staining and PNA binding showed that although there was no axial difference in the percentage of IC (~40%), the fraction of IC which bound PNA was significantly higher in the outer than in the inner cortex (47% vs. 32%, respectively) (Emmons et al., 1991). In a recent study using anti-H^+-ATPase and anti-band-3 immunocytochemistry, and PNA binding, (Schuster et al., 1991) ~20% of all ICs in the rabbit CCD had apical H^+-ATPase with basal band-3 (active type A-IC), ~20% had diffuse H^+-ATPase with basal band-3 staining (presumably resting type A-IC), and the remaining 60% of the CCD- IC were band-3 negative (possibly type B-IC). When they combined anti-H^+-ATPase staining and PNA binding, 66% of IC had diffuse H^+-ATPase staining and bright apical PNA binding, another 9% showed diffuse H^+-ATPase staining with weak apical PNA binding (total of 75% with type B configuration).

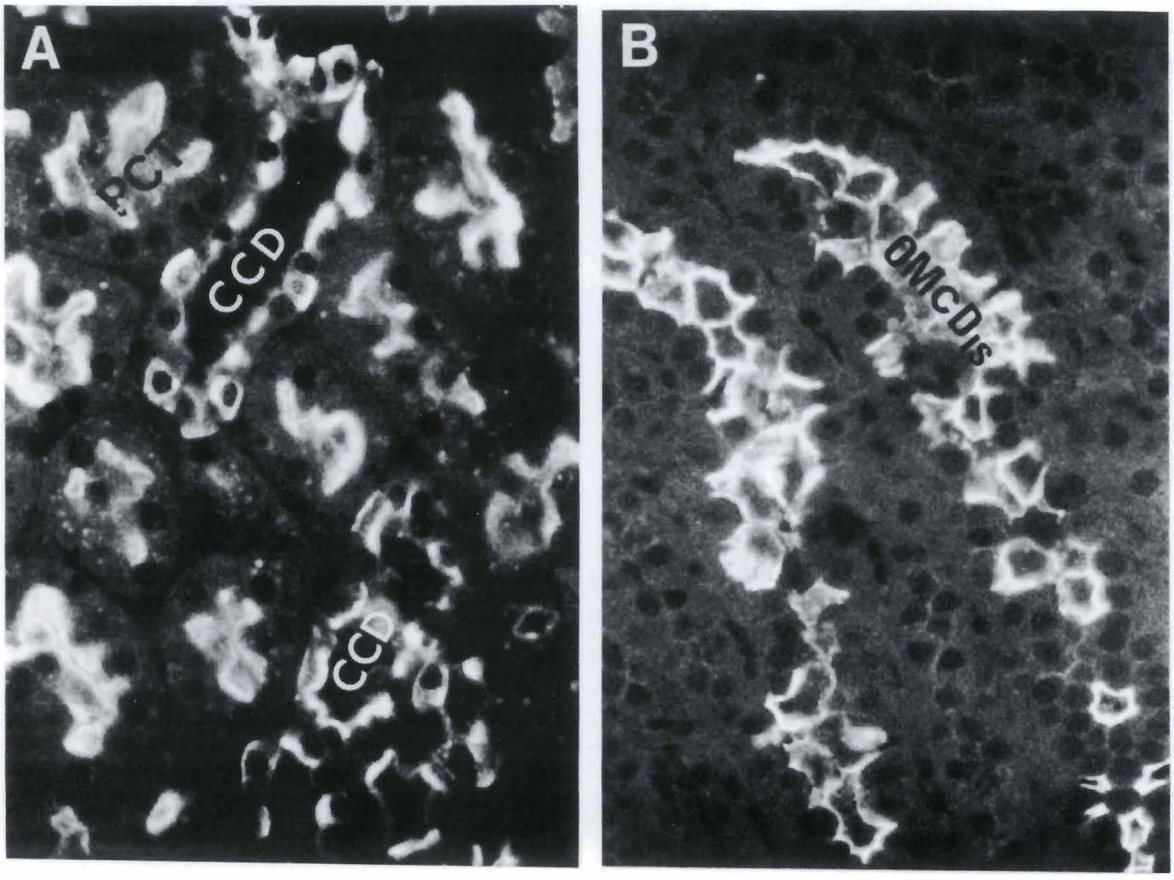

Fig. 4. Rats fed a K^+-depleted diet for two weeks. **A.** In the CCD a higher percentage of IC show well polarized apical (WPA) or well polarized basolateral (WPB) morphology. **B.** In the OMCDIS all IC show a very bright H^+-ATPase staining of the expanded luminal plasma membranes, with total disappearance of the vesicular cytoplasmic H^+-ATPase staining. x 400

Furthermore, 13% of IC had both apical H⁺-ATPase and bright apical PNA binding, 5% had diffuse H⁺-ATPase staining and no PNA binding, 4% had bright PNA binding with no H⁺-ATPase staining, and only 2% had characteristics previously considered classic for type A-IC (i.e., apical H⁺-ATPase with no PNA binding). Moreover, approximately 10% of all PNA positive cells were also band-3 positive. They also found an inverse correlation between band-3 positivity and the intensity of PNA binding, so that only ~4% of IC with strong PNA binding had band-3 staining whereas, 19% of IC with weak PNA binding had band-3 staining. The IC with these non-classic patterns of staining for H⁺-ATPase, band-3 protein, and PNA binding were classified as "hybrid cells" (Schuster et al., 1991). Another interesting finding in the study was that, in contrast to the rat CCD, no IC in the rabbit CCD showed a well polarized basolateral H⁺-ATPase staining. These observations have been expanded further by an ultrastructural localization study using a polyclonal antibody against the 70 kD subunit of bovine brain H⁺-ATPase (Verlander et al., 1994). In that study, three patterns of H⁺-ATPase distribution were identified in IC. The majority of IC were small, lacked distinctive ultrastructural features of either type A or type B cells, and had H⁺-ATPase associated solely with the cytoplasmic vesicles. Within this group some cells had numerous H⁺-ATPase labeled apical cytoplasmic vesicles that could represent inactive or resting type A-IC. The second most frequent pattern consisted of H⁺-ATPase labeling of the basolateral plasma membrane and cytoplasmic vesicles distributed throughout the cell, consistent with type B configuration. The third pattern which was least frequent consisted of H⁺-ATPase labeling of the apical plasma membrane and apical cytoplasmic vesicles, typical for type A-IC (Verlander et al., 1994). In support of these unusual morphologic and immunocytochemical patterns of IC in the rabbit CCD, there are functional studies indicating that a substantial number of IC in this segment carry Cl^-:HCO_3^- anion exchanger in both apical and basolateral plasma membranes (Emmons and Kurtz, 1994; Weiner et al., 1994). Collectively these morphologic, immunocytochemical, and functional studies indicate that the majority of IC in the outer CCD of rabbit have a "hybrid" configuration with a mixture of features of type A and type B cells, and only a few IC show the classic features of either type A or type B cells as shown in the rat CCD. However, in the inner CCD, close to the juxtamedullary region and in the medullary rays, a higher percentage of IC show features of type A cells, with a proportional reduction in the percentage of IC showing features of type B or "hybrid" cells.

On immunocytochemical localization studies of rabbit kidney using anti-31kD monoclonal antibody, we found that in the outer CCD the majority of IC were large with diffuse H⁺-ATPase staining, in many of which the staining was accentuated in basolateral or both basolateral and apical poles (Fig. 5). Approximately 25% of IC had PPA configuration, ~2% WPA, and only 0.2% WPB morphologic configurations. In the inner

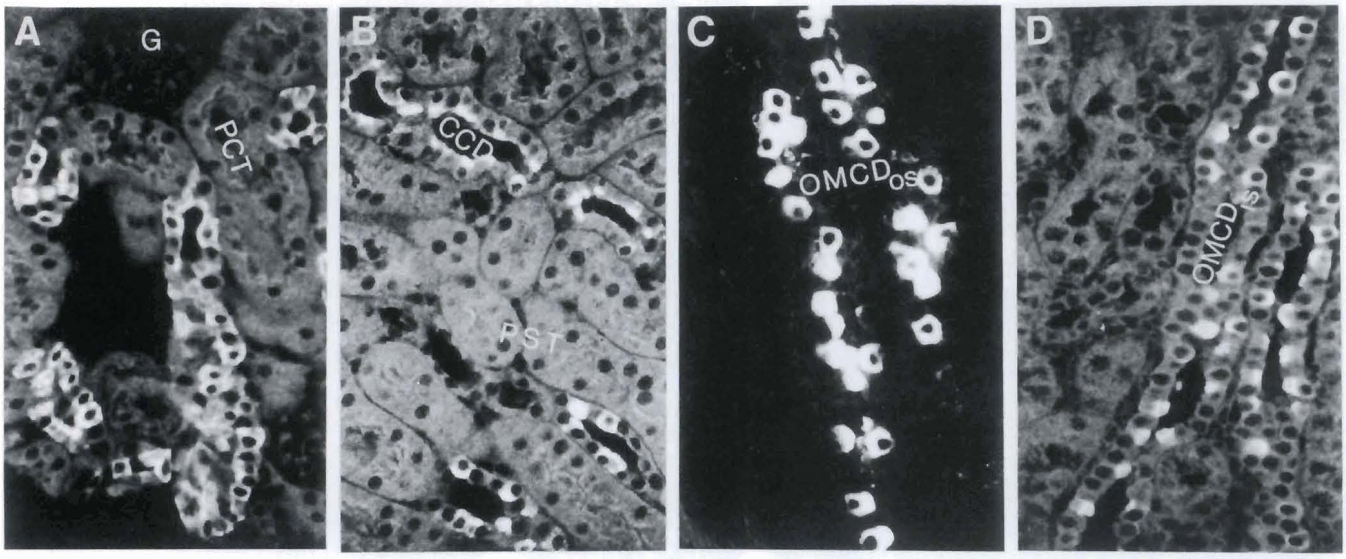

Fig. 5. The rabbit kidney immunostained with a monoclonal antibody against the 31 kD subunit of H⁺-ATPase. **A.** Outer cortex. In the outer CCD, majority of IC show a diffuse H⁺-ATPase staining, with staining frequently accentuated in basal or apical and basal poles. Only an occasional IC shows a more prominent H⁺-ATPase staining in the apical pole. PC do not show any H⁺-ATPase staining. The PCT show only a faint linear pattern of stianing in the apical pole which represents the subvillar invagination staining. The glomerulus (G) shows no H⁺-ATPase staining. **B.** Inner cortex, medullary rays. In the inner CCD, majority of IC show apical polarization for H⁺-ATPase staining. The PST show a very faint subvillar invagination or no H⁺-ATPase staining **C.** Outer stripe of the otuer medulla. IC in the outer medullary collecting duct-outer stripe (OMCDOS) show either PPA or diffuse, and only occasionally a WPA pattern of H⁺-ATPase staining. **D.** Inner stripe of the outer medulla. IC in the outer medullary collecting duct-inner stripe ($OMCD_{IS}$) show predominently a PPA and occasionally a WPA pattern of H⁺-ATPase staining x 250

CCD, in the medullary rays, there was a significant reduction in the percentage of IC showing diffuse, with either basal or bipolar accentuation, H^+-ATPase staining. This was accompanied with a proportional increase in the percentage of IC showing type A configuration (Fig. 5).

Outer medullary collecting duct

The outer medullary collecting duct (OMCD) resides in the outer and inner stripes (OMCDOS, OMCDIS) of the outer medulla. Approximately 60% of the cells in this segment are PCs which are responsible for water homeostasis but no sodium reabsorption. Transport studies in isolated in-vitro perfused collecting duct segments have provided evidence that the OMCD is a major site of proton secretion in the collecting duct (Atkins and Burg, 1985). In the OMCDOS ~90% of IC are type A and the remaining ~10% are either type B or show a diffuse H^+-ATPase staining (Fig. 2) (Alpern et al., 1989; Bastani et al., 1991). In the OMCDIS, based on both H^+-ATPase and band-3 immunocytochemistry, 100% of IC are type A-IC (Fig. 2) (Alpern et al., 1989; Bastani et al., 1991). In experiments in which rats were acid-loaded, with oral NH_4Cl for up to two weeks, we observed a striking adaptational change in the immunocytochemical distribution of H^+-ATPase in IC of the OMCD. In response to chronic acid-loading, many of the IC in this nephron segment showed nearly complete loss of their vesicular cytoplasmic H^+-ATPase staining, with all of the label appearing in the plasma membrane, a pattern we referred to as "rim staining" (Fig. 6) (Bastani et al., 1991). The OMCDIS had the most striking response. The percentage of rim cells increased from 7% to 63% of ICs only after one day, with further increase to 89% over the ensuing two weeks. In the OMCDOS the percentage of rim cells increased from 2% to 25% of IC after one day and to 68% by the end of the two weeks of acid-loading. Ultrastructural and morphometric studies of the OMCD have also shown that during acute respiratory acidosis and chronic metabolic acidosis, IC respond with an increase in the surface density of the apical plasma membrane and a concurrent decrease in the number of apical cytoplasmic tubulovesicular membrane structures (Madsen and Tisher, 1984; Verlander et al., 1987; Madsen et al., 1991). Collectively, these studies highly suggest that IC of the OMCD participate in acidification of the tubule

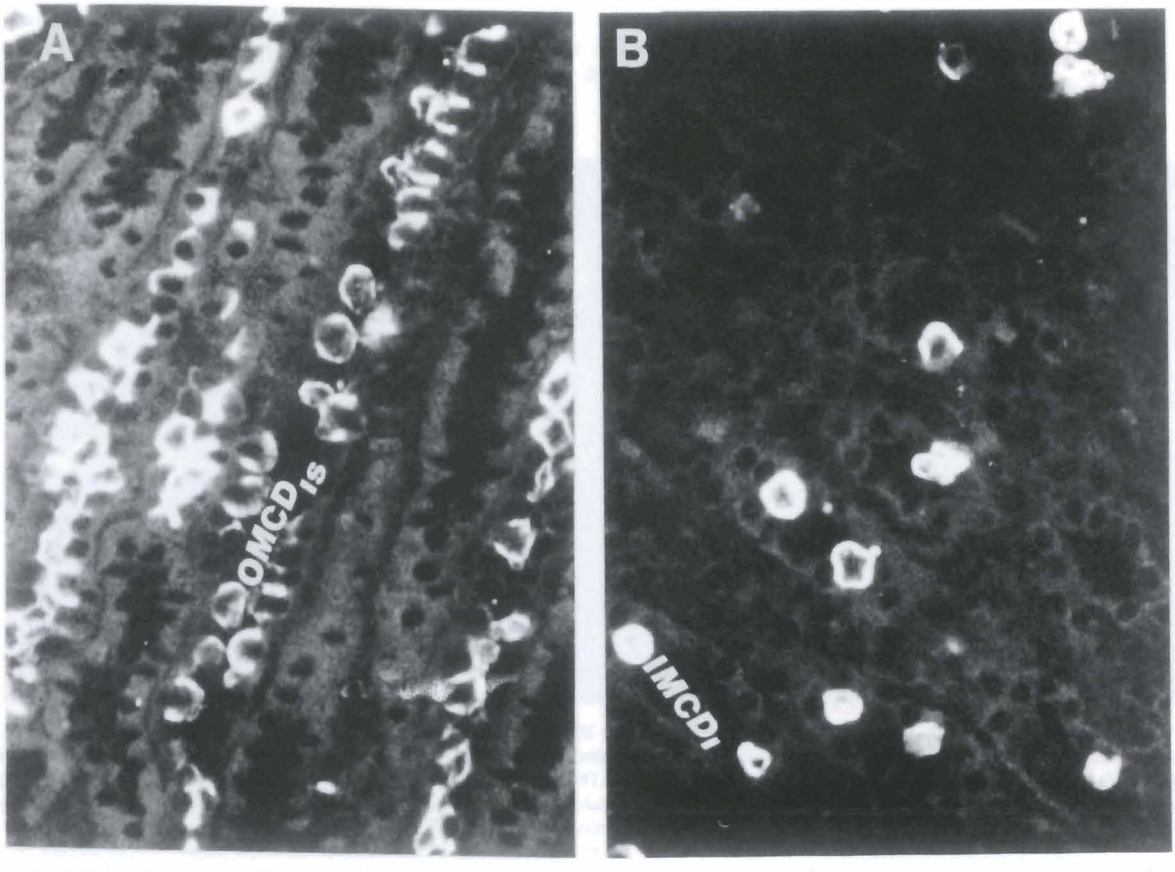

Fig. 6. After two weeks of oral acid-loading with NH_4Cl in drinking water, IC in the medullary collecting duct show very prominent H^+-ATpase staining in the luminal plasma membrane (rim pattern) with almost total absence of H^+-ATpase staining in the cytoplasmic vesicles. This represents redistribution of the H^+-ATPase pump from cytoplasmic vesicles into the luminal plasma membrane leading to significant expansion of the luminal membrane and appearance of the rim cells. **A.** Inner stripe of the outer medulla (OMCDIS). **B.** Initial one-third of the inner medulla (IMCDI). x 400

fluid and that acidosis enhances this acidification by inserting cytoplasmic membrane vesicles containing proton pumps into the apical plasma membrane.

We have found similar adaptive changes in the distribution of the H^+-ATPase pumps from cytoplasmic vesicles to the apical plasma membrane, with the appearance of rim cell, in the remnant kidney model of 7/8 nephrectomy (Fig. 3) and respiratory acidosis (Bastani et al., 1990, 1993). Interestingly, in rats fed a K^+-depleted diet for two weeks, we found the most striking appearance of rim cells in the OMCD, particularly in the inner stripe, to the point that lumen of the tubules were totally occluded with expanded luminal membranes of IC which showed prominent plasma membrane staining (our unpublished observation, Fig. 4). The changes observed with K^+-depleted diet were much more striking than with respiratory acidosis or in the remnant kidney (7/8 nephrectomy) model, and were at least on par with chronic acid-load experiments. This suggested that both H^+-ATPase and H^+,K^+-ATPase pumps are carried in the same tubulovesicular structures in the apical cytoplasm and that K^+-depleted diet, similar to chronic acid-loads, will result in redistribution and fusion of the same apical cytoplasmic vesicles with the luminal plasma membrane.

In the rabbit OMCDOS, IC comprise ~30% and PC comprise the remaining ~70% of the cells. Virtually all of the IC in this segment show basolateral membrane staining for band-3 like protein, with one-half of them demonstrating apical H^+-ATPase (presumably active type A-IC), and the other one-half demonstrating diffuse H^+-ATPase (presumably quiescent type A-IC) immunostaining (Schuster et al., 1986, 1991). Moreover, it has been shown that only one-half of the IC from control rabbit OMCDOS endocytose macromolecules, suggesting that at baseline state only one-half of the type A-IC in this segment are in an active proton secreting state (Schwartz et al., 1988). On immunocytochemical staining of the rabbit kidney using a monoclonal antibody against the 31 kD subunit of H^+-ATPase, IC in the OMCDOS show very bright staining predominantly in PPA or diffuse, and only occasionally in WPA, configuration (Fig. 5).

The rabbit OMCDIS has been claimed to be different from the rat, since only the initial one-half of this segment in the rabbit was shown to contain IC, comprising 10% of cells in the early half (Madsen et al., 1989). A study using succinic dehydrogenase histochemistry to identify IC and anti-band-3 immunoreactivity and PNA binding to identify subtypes of IC, has shown that 40-50% of cells in the rabbit OMCDIS are IC, all of which show basolateral band-3 immunoreactivity and lack apical PNA binding indicative of type A-IC (Schuster et al., 1986). More recently, an immunocytochemical study using anti-H^+-ATPase and anti-band-3 antibodies has revealed that ~90% of IC in this segment have apical H^+-ATPase and basal band-3 staining (active type A-IC morphology), ~8% have diffuse H^+-ATPase and basal band-3 immunostaining (quiescent type A-IC morphology), and ~2% have either apical H^+-ATPase with no basal band-3 or basal band-3 without apical H^+-ATPase staining (Schuster et al., 1991). On immunocytochemical studies using a monoclonal antibody against the 31 kD subunit of H^+-ATPase, 30-35% of cells along the OMCDIS are IC with bright H^+-ATPase staining (Fig. 5). The PC show no H^+-ATPase staining. The IC in the OMCDIS predominantly show a PPA morphology with an occasional IC showing a prominent luminal membrane staining as well. We found a significant reduction in the abundance of IC along the OMCDIS as they approached the inner medulla, although they did not totally disappear.

Inner medullary collecting duct

The inner medullary collecting duct (IMCD) resides in the papillary medulla and is divided into two subsegments: the IMCDI (the initial one-third to one-half) and IMCDT (the terminal one-half to two-thirds). In the rat IMCD, type A-IC are present only in the IMCDI and their prevalence rapidly declines from 30-40% at the junction of OMCD to 0% by the end of the IMCDI. The remaining cells in IMCDI are PC with features similar to their counterparts in the OMCD. The IMCDT is composed of a single cell type, the IMCD cells, which contain both sodium and water channels.

On immunocytochemical staining of rat kidney using a monoclonal antibody against the 31 kD subunit of H^+-ATPase, we found typical IC present only in the IMCDI, some of which showed a prominent luminal membrane staining for H^+-ATPase (Fig. 2C). In experiments in which rats were induced to have chronic metabolic acidosis (oral NH_4Cl feeding), or acute or chronic respiratory acidosis (6 hours or 5 days exposure to 10% CO_2 in air) we found a significant increase in the percentage of IC showing prominent luminal membrane staining for H^+-ATPase (Fig. 6B) (Bastani et al., 1993, 1994).

Acknowledgments. The author wishes to thank Ms. Laura Furdek for her secretarial assistance in preparing this manuscript.

References

Ait-Mohamed A.K., Marsy S., Barlet C., Khadouri C. and Doucet A. (1986). Characterization of N- ethylmaleimide-sensitive proton pump in the rat kidney. J. Biol. Chem. 261, 12526-12533.

Alpern R.J. (1990) Cellular mechanisms of proximal tubule acidification. Physiol. Rev. 70, 79-114.

Alpern S., Natale J., Gluck S., Lodish H. and Brown D. (1989). Intercalated cell subtypes in rat kidney collecting duct defined using antibodies against erythrocyte band 3 and renal vacuolar H^+-ATPase. Proc. Natl. Acad. Sci. USA 86, 5429-5433.

Atkins J.L. and Burg M.B. (1985) Bicarbonate transport by isolated perfused rat collecting ducts. Am. J. Physiol. 249, F485-F496.

Bank N., Aynedjian H.S. and Mutz B.F. (1989). Proximal bicarbonate absorption independent of Na^+- H^+ exhange: effect of bicarbonate

load. Am J . Physiol. 256, F577-F582.

Bastani B. (1995). Colocalization of H-ATPase and H,K-ATPase immunoreactivity in the rat kidney. J. Am. Soc. Nephrol. 5, 1476-1482.

Bastani B. and Gluck S. (1992). Chronic DOCA induces changes in vacuolar H^+-ATPase quantity and distribution in rat kidney. J. Am. Soc. Nephrol. 3, 772A.

Bastani B., Hemken P. and Gluck S. (1990). Adaptation of renal vacuolar H^+ATPase in rat remnant kidney model. J. Am. Soc. Nephrol . 1, 646A.

Bastani B., Purcell H., Hemken P., Trigg D. and Gluck S. (1991). Expression and distribution of renal vacuolar proton-translocating adenosine triphosphatase in response to chronic acid and alkali loads in the rat. J. Clin. Invest. 88, 126-136.

Bastani B., Gluck S., Hilden S., Johns C., Yang L. and Madias N. (1993). Adaptation of renal vacuolar H^+-ATPase to acute or chronic respiratory acidosis in the rat. J. Am. Soc. Nephrol. 4, 831A.

Bastani B., McEnaney S., Yang L. and Gluck S. (1994a). Adaptation of inner medullary collecting duct vacuolar H-adenosine triphosphatase to chronic acid or alkali loads in the rat. Exp. Nephrol. 2, 171-175.

Bastani B., Yang L. and Steinhardt G. (1994b). Immunocytochemical localization of vacuolar H^+-ATPase in the opossum (*Monodelphis domestica*) kidney: Comparison with the rat. J. Am. Soc. Nephrol. 4, 1558-1563.

Brown D., Gluck S. and Hartwig J. (1987). Structure of the novel membrane-coating material in proton-secreting epithelial cells and identification as an H^+-ATPase. J Cell Biol. 105, 1637-1648.

Brown D., Hirsch S., Gluck S. (1988a). Localization of a proton-pumping ATPase in rat kidney. J. Clin. Invest. 82, 2114-2126.

Brown D., Hirsch S. and Gluck S. (1988b). An H^+ATPase in opposite plasma membrane domains in kidney epithelial cell subpopulations. Nature 331, 622-624.

Borensztein P., Leviel F., Froissart M., Houillier P., Poggioli J., Marty E., Bichara M. and Paillard M. (1991). Mechanisms of H^+/HCO_3^- transport in the medullary thick ascending limb of rat kidney. Kidney Int. 33, S43-S46.

Brosius F.C., Alper S.L., Garcia A.M. and Lodish H.F. (1989) The major kidney transcript preducts an amino-terminal truncated band 3 polypeptide. J. Biol. Chem. 264, 7784-7787.

Doucet A., Khadouri C., Chevel L., Marsy S. and Barlet-Bas C. (1993). Renal proton adenosine triphosphatases. Adv. Nephrol. 22, 287-304.

Emmons C. and Kurtz I. (1994). Functional characterization of three intercalated cell subtypes in the rabbit outer cortical collecting duct. J Clin. Invest. 93, 417-423.

Emmons C.L., Matsuzaki K., Stokes J.B. and Schuster V.L. (1991). Axial heterogeneity of rabbit cortical collecting duct. Am.J. Physiol. 260, F498-F505.

Forgac M. (1992). Structure, function and regulation of the coated vesicle V-ATPase. J. Exp. Biol. 172, 155-169.

Garg L.C. (1991). Respective roles of H^+-ATPase and H^+,K^+-ATPase in ion transport in the kidney. J. Am. Soc. Nephrol. 2, 949-960.

Gluck S. (1992). The structure and biochemistry of the vacuolar H-ATPase in proximal and distal urinary acidifcation. J. Bioenerg. Biomembr. 24, 351-359.

Gluck S. (1993). The Vacuolar H^+ATPases: Versatile proton pumps participating in constitutive and specialized functions of eukaryotic cells. Int. Rev. Cytol. 137C, 105-137.

Gluck S., Kelly S. and Al-Awqati Q. (1982). The proton translocating ATPase responsible for urinary acidification. J. Biol. Chem. 257, 9230-9233.

Gluck S., Bastani B., Nelson R., Purcell H., Wang Z-Q., Zhang K., Marushak M., Lee B., Guo X-L., Masood K. and Hemken P. (1991). Properties and function of the kidney vacuolar H-ATPase: A versatile proton pump responsible for urinary acidification. Proc. XI Int. Cong. Nephrol. Tokyo Japan. Vol 1: Nephrol. Hatano M. (ed). Springer- Verlag. pp 435-444.

Gluck S.L., Nelson R.D. and Lee B.S. (1993). Properties and regulation of the renal vacuolar H^+-ATPase and H^+,K^+-ATPase. Curr. Opin. Nephrol. Hyperten. 2, 715-724.

Hamm L.L., Weiner I.D. and Vehaskari V.M. (1991). Structural-functional characteristics of acid-base transport in the rabbit collecting duct. Semin. Nephrol. 11, 453-464.

Hemken Ph., Xiao-Li G., Zhi-Qiang W., Kun Z. and Gluck S. (1992). Immunologic evidence that vacuolar H^+-ATPase with heterogeneous forms of Mr = 31,000 subunit have different membrane distribution in mammalian kidney. J. Biol. Chem. 267, 9948-9957.

Lombard W.E., Kokko J.P. and Jacobsen H.R. (1983). Bicarbonate transport in cortical and outer medullary collecting tubules. Am. J . Physiol. 244, F289-F296.

Madsen K.M. and Tisher C.C. (1984). Response of intercalated cells of rat outer medullary collecting duct to chronic metabolic acidosis. Lab. Invest. 51, 258-276.

Madsen K.M., Verlander J.W. and Linser P.J. (1989). Identification of intercalated cells in rabbit medullary collecting duct. Kidney Int. 35, 458A.

Madsen K.M., Verlander J.W., Kim J. and Tisher C.C. (1991). Morphological adaptation of the collecting duct to acid-base disturbances. Kidney Int. (Suppl.) 33, S57-S63.

Madsen K.M., Kim J. and Tisher C.C. (1992). Intracellular band-3 immunostaining in type A intercalated cells of rabbit kidney. Am. J. Physiol. 262, F1015-F1022.

McKinney T.D and Burg M.B (1977). Bicarbonate transport by rabbit cortical collecting tubules: Effect of acid and alkali loads in vivo on transport in vitro. J. Clin. Invest. 60, 766-768.

McKinney T.D. and Burg M.B. (1978a). Bicarbonate secretion by rabbit cortical collecting tubules in vitro. J Clin. Invest. 61, 1421-1427.

McKinney T.D. and Burg M.B. (1978b). Bicarbonate absorption by rabbit cortical collecting tubules in vitro. Am. J Physiol. 234, F141-F145.

Muto S., Yasoshima K., Yoshitomi K., Imai M. and Asano Y. (1990). Electrophysiological idenitification of a- and b- intercalated cells and their distribution along the rabbit distal nephron segments. J Clin. Invest. 86, 1829-1839.

Nelson R.D., Guo X.L., Masood K., Brown D., Kalkbrenner M. and Gluck S. (1992). Selectively amplified expression of an isoform of the vacuolar H^+-ATpase 56-kilodalton subunit in renal intercalated cells. Proc. Natl. Acad. Sci. USA 89, 3541-3545.

Preisig P.A., Ives H.E., Cragoe E.J, Alpern R.J. and Rector F.C. (1987). Role fo the Na^+/H^+ antiporter in rat proximal tubule bicarbonate absorption. J. Clin. Invest. 80, 970-978.

Schuster V.L. (1991). Cortical collecting duct bicarbonate secretion. Kidney Int (Suppl). 33, S47-S50.

Schuster V.J. Onsib S.M. and Jennings M.L. (1986). Two types of collecting duct mitochondria-rich (intercalated) cells: lectin and band-3 cytochemistry. Am. J. Physiol. 251, C347-C355.

Schuster V.L., Fejes-Toth G., Narary-Fejes-Toth A. and Gluck S. (1991). Colocalization of H^+-ATPase and band 3 anion exchanger in rabbit

collecting duct intercalated cells. Am. J. Physiol. 260, F506-F517.

Schwartz G.J. and Al-Awqati Q. (1985). Carbon dioxide causes exocytosis of vesicles containing H^+ pumps in isolated perfused proximal and collecting tubules. J Clin. Invest. 75, 1638-1644.

Schwartz G.J., Satlin L.M. and Bergmann J.E. (1988). Fluorescent characterization of collecing duct cells: A second H^+-secreting type. Am. J. Physiol. 255, F1003-F1014.

Simon B.J. and Burckhardt G. (1990). Characterization of inside-out oriented H^+-ATPases in cholate- pretreated renal brush border membrane vesicles. J. Membr. Biol. 1990, 117, 141-151.

Soleimani M., Bookstein C., Singh G., Rao M.C., Chang E.B. and Bastani B. (1995). Differential regulation of Na^+/H^+ exchange and H^+-ATPase by pH and HCO_3^- in kidney. J. Membr. Biol. 144, 209-216.

Turrini F., Sabolic I., Zimolo Z., Moewes B. and Burckhardt G. (1989). Relation of ATPase in rat renal brush border membranes to ATP-drive H^+ secretion. J. Membr. Biol. 107, 1-12.

Verlander J.W., Madsen K.M. and Tisher C.C. (1987). Effect of acute respiratory acidosis on two populations of intercalated cells in rat cortical collecting duct. Am. J. Physiol. 253, F1142-F1156.

Verlander J.W., Madsen K.M., Low P.S., Allen D.P. and Tisher C.C. (1988). Immunocytochemical localization of band-3 protein in the rat collecting duct. Am. J. Physiol. 255, F115- F125.

Verlander J.W., Madsen K.M. and Tisher C.C. (1991). Structural and functional features of proton and bicarbonate transport in the rat collecting duct. Semin. Nephrol. 11, 465-477.

Verlander J.W., Madsen K.M., Stone D.K. and Tisher C.C. (1994) Ultrastructural localization of H^+-ATPase in rabbit cortical collecting duct. J. Am. Soc. Nephrol. 4, 1546-1557.

Wang Z.Q. and Gluck S. (1990). Isolation and properties of bovine kidney brush border vacuolar H^+-ATPase: a proton pump with enzymatic and structural differences from kidney microsomal H^+-ATPases. J Biol. Chem. 265, 21957-21965.

Weiner I.D., Weill A.E. and New A.R. (1994). Distribution of Cl^-/HCO_3^- exchange and intercalated cells in rabbit cortical collecting duct. Am. J. Physiol. 267, F952-F964.